J|A|C|S ARTICLES

Published on Web 12/19/2008

Single Nanowire on a Film as an Efficient SERS-Active Platform

Ilsun Yoon,[†] Taejoon Kang,[†] Wonjun Choi,[‡] Jangbae Kim,[†,§] Youngdong Yoo,[†] Sang-Woo Joo,[||] Q-Han Park,[‡] Hyotcherl Ihee,*[,†,§] and Bongsoo Kim*[,†]

Department of Chemistry, KAIST, Daejeon 305-701, Korea, Department of Physics, Korea University, Seoul 136-701, Korea, Center for Time-Resolved Diffraction, KAIST, Daejeon 305-701, Korea, and Department of Chemistry, Soongsil University, Seoul 156-743, Korea

Received September 19, 2008; E-mail: hyotcherl.ihee@kaist.ac.kr; bongsoo@kaist.ac.kr

Abstract: Fabricating well-defined and highly reproducible platforms for surface-enhanced Raman scattering (SERS) is very important in developing practical SERS sensors. We report a novel SERS platform composed of a single metallic nanowire (NW) on a metallic film. Optical excitation of this novel sandwich nanostructure provides a line of SERS hot spots (a SERS hot line) at the gap between the NW and the film. This single nanowire on a film (SNOF) architecture can be easily fabricated, and the position of hot spots can be conveniently located in situ by using an optical microscope during the SERS measurement. We show that high-quality SERS spectra from benzenethiol, brilliant cresyl blue, and single-stranded DNA can be obtained on a SNOF with reliable reproducibility, good time stability, and excellent sensitivity, and thus, SNOFs can potentially be employed as effective SERS sensors for label-free biomolecule detection. We also report detailed studies of polarization- and material-dependent SERS enhancement of the SNOF structure.

Introduction

Surface-enhanced Raman scattering (SERS) is a fascinating phenomenon that enormously increases Raman signals (by a factor of up to 10^{14}) compared with normal Raman signals. This spectacular enhancement, caused by the strong light-induced electric field at locations in the metallic nanostructured space (usually called hot spots), makes SERS an attractive detection method with high sensitivity and selectivity for the analytes of interest.[1−5] It is known that the SERS enhancement strongly depends on the detailed morphology of the metal nanostructure. While a number of promising nanostructures that can be used as efficient SERS-active platforms have been proposed, such as nanowire (NW) bundles, nanoshells, nanoprisms, and nanoparticle (NP) sandwich nanostructures,[6−35] constructing highly regular and reproducible SERS hot spots still remains a challenging task. Fabrication of such SERS-active platforms that have well-defined and reproducible structures is greatly desirable

[†] Department of Chemistry, KAIST.
[‡] Korea University.
[§] Center for Time-Resolved Diffraction, KAIST.
[||] Soongsil University.

(1) Moskovits, M. *Rev. Mod. Phys.* **1985**, *57*, 783.
(2) Jeanmaire, D. L.; Van Duyne, R. P. *J. Electroanal. Chem. Interfacial Electrochem.* **1977**, *84*, 1.
(3) Nie, S.; Emory, S. R. *Science* **1997**, *275*, 1102.
(4) Kneipp, K.; Kneipp, H.; Itzkan, I.; Dasari, R. R.; Feld, M. S. *Chem. Rev.* **1999**, *99*, 2957.
(5) Kneipp, K.; Kneipp, H.; Kneipp, J. *Acc. Chem. Res.* **2006**, *39*, 443.
(6) Tian, Z.-Q.; Ren, B.; Wu, D.-Y. *J. Phys. Chem. B* **2002**, *106*, 9463.
(7) Tian, J.-H.; Liu, B.; Li, X.; Yang, Z.-L.; Ren, B.; Wu, S.-T.; Tao, N.; Tian, Z.-Q. *J. Am. Chem. Soc.* **2006**, *128*, 14748.
(8) Lu, Y.; Liu, G. L.; Lee, L. P. *Nano Lett.* **2005**, *5*, 5.
(9) McLellan, J. M.; Li, Z.-Y.; Siekkinen, A. R.; Xia, Y. *Nano Lett.* **2007**, *7*, 1013.
(10) Wiley, B. J.; Chen, Y.; McLellan, J. M.; Xiong, Y.; Li, Z.-Y.; Ginger, D.; Xia, Y. *Nano Lett.* **2007**, *7*, 1032.
(11) Imura, K.; Okamoto, H. *Bull. Chem. Soc. Jpn.* **2008**, *81*, 659.
(12) Brolo, A. G.; Arctander, E.; Gordon, R.; Leathem, B.; Kavanagh, K. L. *Nano Lett.* **2004**, *4*, 2015.
(13) Ringler, M.; Klar, T. A.; Schwemer, A.; Susha, A. S.; Stehr, J.; Raschke, G.; Funk, S.; Borowski, M.; Nichtl, A.; Kürzinger, K.; Phillips, R. T.; Feldmann, J. *Nano Lett.* **2007**, *7*, 2753.
(14) Svedberg, F.; Li, Z.; Xu, H.; Käll, M. *Nano Lett.* **2006**, *6*, 2639.
(15) Imura, K.; Okamoto, H.; Hossain, M. K.; Kitajima, M. *Nano Lett.* **2006**, *6*, 2173.
(16) Jeong, D. H.; Zhang, Y. X.; Moskovits, M. *J. Phys. Chem. B* **2004**, *108*, 12724.
(17) Tao, A. R.; Kim, F.; Hess, C.; Goldberger, J.; He, R.; Sun, Y.; Xia, Y.; Yang, P. *Nano Lett.* **2003**, *3*, 1229.
(18) Jackson, J. B.; Halas, N. J. *Proc. Natl. Acad. Sci. U.S.A.* **2004**, *101*, 17930.
(19) Talley, C. E.; Jackson, J. B.; Oubre, C.; Grady, N. K.; Hollars, C. W.; Lane, S. M.; Huser, T. R.; Nordladner, P.; Halas, N. J. *Nano Lett.* **2005**, *5*, 1569.
(20) Qin, L.; Zou, S.; Xue, C.; Atkinson, A.; Schatz, G. C.; Mirkin, C. A. *Proc. Natl. Acad. Sci. U.S.A.* **2006**, *103*, 13300.
(21) Willets, K. A.; Van Duyne, R. P. *Annu. Rev. Phys. Chem.* **2007**, *58*, 267.
(22) Zhang, X.; Zhao, J.; Whitney, A. V.; Elam, J. W.; Van Duyne, R. P. *J. Am. Chem. Soc.* **2006**, *128*, 10304.
(23) Stuart, D. A.; Yuen, J. M.; Shat, N.; Lyandres, O.; Yonzon, C. R.; Glucksberg, M. R.; Walsh, J. T.; Van Duyne, R. P. *Anal. Chem.* **2006**, *78*, 7211.
(24) Sawai, Y.; Takimoto, B.; Nabika, H.; Ajito, K.; Murakoshi, K. *J. Am. Chem. Soc.* **2007**, *129*, 1658.
(25) Camden, J. P.; Dieringer, J. A.; Wang, Y.; Masiello, D. J.; Marks, L. D.; Schatz, G. C.; Van Duyne, R. P. *J. Am. Chem. Soc.* **2008**, *130*, 12616.
(26) Nordlander, P.; Le, F. *Appl. Phys. B: Lasers Opt.* **2006**, *84*, 35.
(27) Zheng, J.; Zhou, Y.; Li, X.; Ji, Y.; Lu, T.; Gu, R. *Langmuir* **2003**, *19*, 632.
(28) Orendorff, C. J.; Gole, A.; Sau, T. K.; Murphy, C. J. *Anal. Chem.* **2005**, *77*, 3261.
(29) Kim, K.; Yoon, J. K. *J. Phys. Chem. B* **2005**, *109*, 20731.

 10.1021/ja807455s CCC: $40.75 © 2009 American Chemical Society

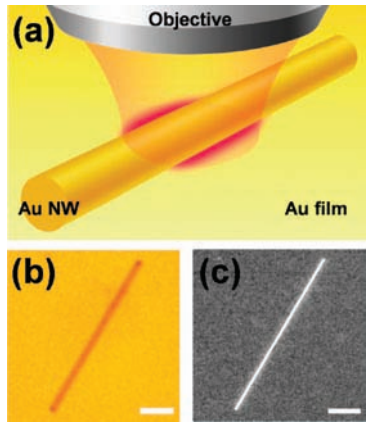

Figure 1. (a) Schematic illustration of a SNOF architecture constructed by placing a Au NW on a Au film. (b) Optical microscope image of a SNOF architecture. (c) SEM image of the SNOF in (b), showing that only a single Au NW is present. The scale bars represent 1 μm.

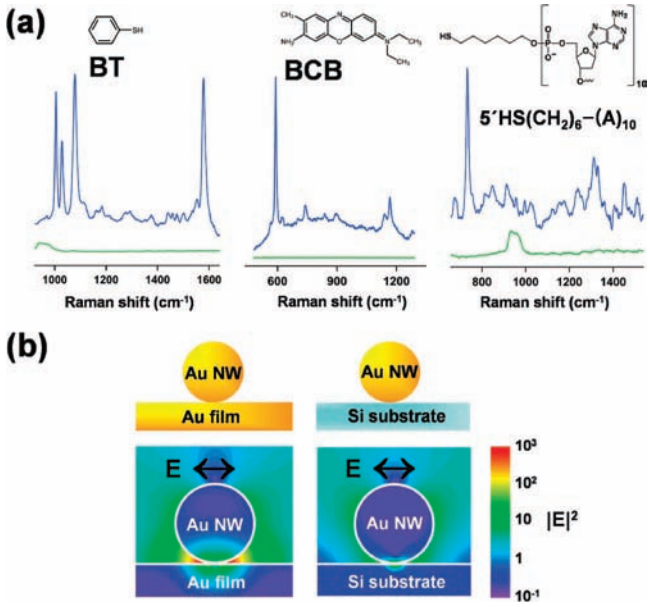

Figure 2. (a) SERS spectra of BT, BCB, and HS-A_{10} for (blue) the Au/Au SNOF system and (green) a Au NW on a Si substrate. The peak near 850 cm^{-1} in the green trace is a Si Raman peak. The polarization of the incident light is perpendicular to the NW axis. (b) Calculated distributions of the local electric field intensities, $|E|^2$, for (left) the Au/Au SNOF and (right) a Au NW on a Si substrate, with an incident light polarization perpendicular to the NW axis.

for developing SERS sensors for efficient biological and medical applications.[36−41]

Here we introduce a novel SERS-active platform composed of a single-crystalline NW and a film that enhances a Raman signal to a level suitable for a practical biosensor. This platform can be generated simply by casting a metallic NW onto a metallic film, thus promising wide applicability. This single nanowire on a film (SNOF) as a sandwich architecture (shown schematically in Figure 1a) provides a line of SERS hot spots (i.e., a SERS hot line) at the gap between the NW and the film upon optical excitation. The exact position of the hot spots can be conveniently located in situ by using an optical microscope during the SERS measurement rather than a scanning electron

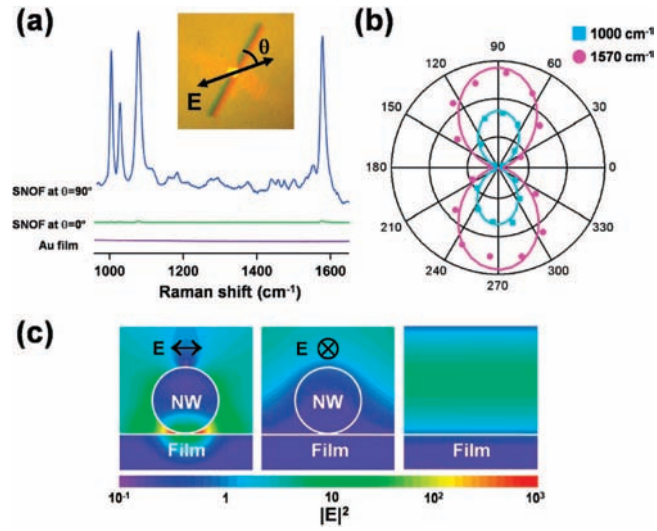

Figure 3. (a) Polarization dependence of the SERS spectra of BT on the Au/Au SNOF. The traces with the polarization of the incident light (blue) perpendicular and (green) parallel to the Au NW were recorded at the same point on the NW. The violet trace was recorded for the flat Au film as a control. (b) Polar plots of the integrated SERS intensities of the (■) 1000 and (●) 1570 cm^{-1} BT Raman bands with respect to θ, the angle between the incident polarization and the NW axis. The cyan and magenta lines represent best fits to $\cos^2\theta$ functions. (c) Distributions of local electric field intensities, $|E|^2$, for a Au/Au SNOF with the light polarization (left) perpendicular and (middle) parallel to the NW axis and (right) for a smooth Au film.

microscope (SEM) or atomic force microscope (AFM) after the SERS measurement.[36]

Au and Ag NWs employed to fabricate SNOF platforms are single-crystalline without twins or defects and have atomistically smooth surfaces. The root-mean-square (rms) roughness of the Au and Ag films was only a few nanometers, providing practically flat surfaces.[30,35] Since the SNOF provides a very simple SERS-active nanostructure that contains only a single NW (one-dimensional) and a flat film (two-dimensional), it can serve as a representative model system for investigating how SERS enhancement between a NW and a film is correlated with surface plasmon excitation in the NW and with the materials composing the SNOF. The experimental SERS enhancements of a SNOF with respect to a single metal NW on a Si substrate and to the metallic film itself are compared to theoretical results obtained using the three-dimensional finite-difference time domain (FDTD) method and show good agreement.

(30) Anderson, D. J.; Moskovits, M. *J. Phys. Chem. B* **2006**, *110*, 13722.
(31) Driskell, J. D.; Lipert, R. J.; Porter, M. D. *J. Phys. Chem. B* **2006**, *110*, 17444.
(32) Evanoff, D. D.; Heckel, J.; Caldwell, T. P.; Christensen, K. A.; Chumanov, G. *J. Am. Chem. Soc.* **2006**, *128*, 12618.
(33) Kinnan, M. K.; Chumanov, G. *J. Phys. Chem. C* **2007**, *111*, 18010.
(34) Wang, Y.; Zou, X.; Ren, W.; Wang, W.; Wang, E. *J. Phys. Chem. C* **2007**, *111*, 3259.
(35) Braun, G.; Lee, S. J.; Dante, M.; Nguyen, T.-Q.; Moskovits, M.; Reich, N. *J. Am. Chem. Soc.* **2007**, *129*, 6378.
(36) Braun, G.; Pavel, I.; Morrill, A. R.; Seferos, D. S.; Bazan, G. C.; Reich, N. O.; Moskovits, M. *J. Am. Chem. Soc.* **2007**, *129*, 7760.
(37) Murphy, C. J.; Sau, T. K.; Gole, A. M.; Orendorff, C. J.; Gao, J.; Gou, L.; Hunyadi, S. E.; Li, T. *J. Phys. Chem. B* **2005**, *109*, 13857.
(38) Liu, G. L.; Lu, Y.; Kim, J.; Doll, J. C.; Lee, L. P. *Adv. Mater.* **2005**, *17*, 2683.
(39) Domke, K. F.; Zhang, D.; Pettinger, B. *J. Am. Chem. Soc.* **2007**, *129*, 6708.
(40) Ren, B.; Picardi, G.; Pettinger, B.; Schuster, R.; Ertl, G. *Angew. Chem., Int. Ed.* **2005**, *44*, 139.
(41) Gunawidjaja, R.; Peleshanko, S.; Ko, H.; Tsukruk, V. V. *Adv. Mater.* **2008**, *20*, 1544.

Table 1. Results from FDTD Calculations Compared with Experimental SERS Intensities of the 580 cm^{-1} Band of BCB for the Au/Au SNOF and Au NW on a Si Substrate Shown in Figure 2

system	integrated FDTD $\|E\|^4$	exptl SERS intensity[a]
Au NW on Si substrate	1.5×10^7	8
Au/Au SNOF	1.7×10^{10}	4120
enhancement factor	1100	520

[a] Arbitrary units.

We also show that high-quality SERS spectra from benzenethiol (BT), brilliant cresyl blue (BCB), and single-stranded DNA (ssDNA) adsorbed onto SNOFs can be obtained with reliable reproducibility, good time stability, and excellent sensitivity. These superb properties can be further applied to biosensors for label-free detection.

Experimental Section

Preparation of Au and Ag NWs and Au and Ag Films. Au NWs were synthesized on a sapphire substrate in a horizontal quartz tube furnace system using a vapor transport method. The sapphire substrate was placed a few centimeters downstream from an alumina boat filled with 0.03 g of pure Au powder as a precursor. No catalyst was used. Ar gas flowed at a rate of 100 sccm, maintaining the chamber pressure at 1−5 Torr. The high-temperature zone of the furnace was heated to 1100 °C. Au NWs were grown on the substrate for ~30 min of reaction time. Figure S1(a) in the Supporting Information shows an SEM image of as-synthesized Au NWs on a sapphire substrate. The Au NWs are single-crystalline and have a diamond-shaped cross section, diameters of 100−200 nm, length of up to tens of micrometers, and atomistically flat facets. Ag NWs were synthesized on a Si substrate using a previously reported vapor transport method.[42] The Ag NWs are single-crystalline and have a round cross section, diameters of 80−150 nm, and lengths of up to tens of micrometers. Smooth Au and Ag films were prepared on precleaned silicon substrates by electron-beam-assisted deposition of 10 nm of Cr followed by 300 nm of Au or Ag. The surfaces of the Au and Ag films were smooth enough to be SERS inactive by themselves, and the rms roughnesses of the films were measured to be 2.3 and 2.8 nm, respectively, using an AFM (see Figure S4 in the Supporting Information) The Au and Ag films were cut to 0.25 cm^2 for SNOF fabrication.

Preparation of SNOFs. To demonstrate improved SERS properties of SNOFs, three molecules with various molecular sizes were tested: BCB, BT, and a thiolated 10-mer adenine ssDNA (HS-A_{10}). The Au NWs were incubated in the solutions containing the analytes under the following conditions: (i) for BCB, Au NWs were incubated for 30 min in a 2 μM BCB solution in ethanol; (ii) for BT, Au and Ag NWs were incubated in a 2 mM BT solution in ethanol for 1 day; (iii) for HS-A_{10}, which was synthesized by GenoTech (Daejeon, Korea), Au NWs were incubated in a 50 μM aqueous solution of HS-A_{10} for 1 day at 20 °C. A drop of the incubated Au NW solution was cast on a Au film. The SNOF was washed several times with pure ethanol (BT) and purged with nitrogen to remove the excess solvent. The NWs were immediately immobilized on the film, constructing the SNOF architecture. A comparison of optical and SEM images of a SNOF structure comprising a Au NW on a flat Au film (a Au/Au SNOF) confirmed that only a single Au NW was present in the SNOF (Figure 1b,c). To quantitatively estimate the SERS enhancements of these SNOF structures, control experiments were done by putting single drops of Au NW solutions of the same analytes on a Si substrate.

Raman Spectroscopy. SERS measurements were performed using a home-built micro-Raman system equipped with a thermo-electrically cooled CCD detector.[42] The NWs were illuminated by the 632.8 nm light of a He−Ne laser. The laser light was linearly polarized, and its polarization direction was controlled by rotating a half-wave plate. The incident laser beam (~500 nm diameter) was focused on the point of the NW of a SNOF structure and the Raman signal from the Au NW collected using the same high-magnification objective. For BCB, a 100× objective (NA = 0.7) was used to collect the Raman signals of the BCB from the Au/Au SNOF and the Au NW on the Si substrate. The NWs were excited by an ~3 μW laser for 1 min. The SERS signal was collected for a dried sample on the SNOF. For BT and HS-A_{10}, a 60× objective (NA = 1.2) was used to collect the Raman signals on the SNOFs, which were excited by the ~300 μW laser for 3 min. SNOF samples were immersed in water.

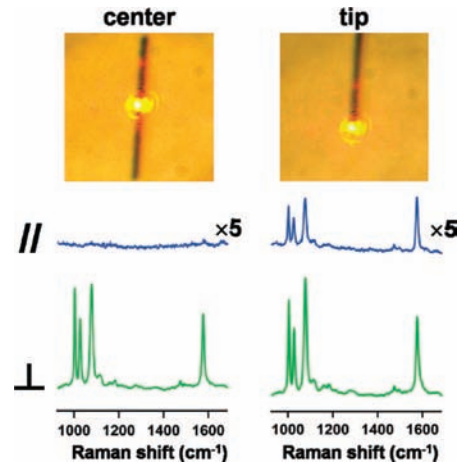

Figure 4. SERS spectra of BT (left) at the center and (right) at the tip of the same NW of the Au/Au SNOF system, with the polarization of the incident laser beam parallel (//) and perpendicular (⊥) to the NW axis.

Table 2. Experimental and Theoretical Polarization-Dependent SERS Intensities of the Au/Au SNOF and the Flat Au Film

system	polarization direction	integrated FDTD $\|E\|^4$	exptl SERS intensity[a]
Au film		6.5×10^5	10[b]
Au/Au SNOF	perpendicular	1.7×10^{10}	1.9×10^4
	parallel	4.6×10^5	57

[a] Peak intensity of BT at 1000 cm^{-1} (Figure 3a) in arbitrary units. [b] The intensity of the noise level.

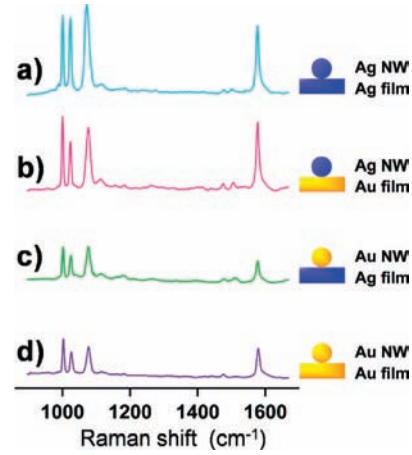

Figure 5. (a) SERS spectra of BT for four different SNOF structures composed of Ag and Au, having (a) Ag/Ag, (b) Ag/Au, (c) Au/Ag, and (d) Au/Au NW/film components. All four spectra are on the same scale. Peaks are observed at the same positions.

(42) Mohanty, P.; Yoon, I.; Kang, T.; Seo, K.; Varadwaj, K. S. K.; Choi, W.; Park, Q.-H.; Ahn, J. P.; Suh, Y. D.; Ihee, H.; Kim, B. *J. Am. Chem. Soc.* **2007**, *129*, 9576.

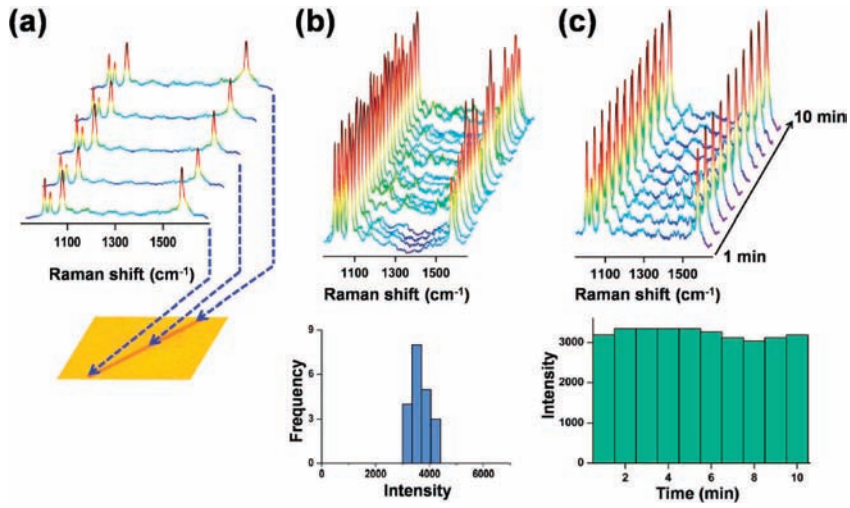

Figure 6. (a) (top) SERS spectra of BT at five different positions on the same Au NW of the Au/Au SNOF structure; (bottom) corresponding positions on the NW. (b) (top) SERS spectra of BT from 20 different single Au NWs of the Au/Au SNOF structure; (bottom) histogram of the intensities of the 1000 cm^{-1} band. (c) (top) SERS spectra of BT as a function of time, recorded at 1 min intervals for 10 min at the same point on a Au/Au SNOF structure; (bottom) time variation of the intensity of the 1000 cm^{-1} band.

Theoretical Calculations. To investigate theoretically the SERS enhancement of the Au/Au SNOF with respect to a single NW on a Si substrate, the FDTD method was employed to calculate the distributions of the local electric field intensities, $|E|^2$, around a single Au NW on a Au film and a single Au NW on a Si substrate at the excitation wavelength of 632.8 nm (Figure 2b). The Au NW placed on a Si substrate or a smooth Au film was locally excited by a Gaussian beam with a diameter (fwhm) of 500 nm and polarization perpendicular or parallel to the NW axis. A realistic dielectric function for Au was used in the calculations. For simplicity, the Au NW was assumed to have a circular cross section with a diameter of 100 nm, and the film was assumed to be flat and 300 nm thick. In these calculations, all of the electric field intensities around the NW were normalized to that of the input Gaussian beam.

Results and Discussion

1. SERS Enhancement of the SNOF. Figure 2a shows the SERS spectra of BCB,[43] BT,[44] and HS-A_{10}[45] adsorbed onto Au/Au SNOF structures and Au NWs on Si substrates. The SERS spectra were taken with the polarization perpendicular to the NW axis. Strong SERS enhancement of the SNOF system with respect to the Au NW on a Si substrate was observed for all three tested molecules.

The distributions of the local electric field intensities, $|E|^2$, around the Au/Au SNOF and a Au NW on a Si substrate were calculated at the excitation wavelength of 632.8 nm (Figure 2b and Figure S5 in the Supporting Information). When the perpendicularly polarized light impinges on the NW, a strongly enhanced electric field (shown in red in the color-gradient scheme) is locally induced at the gap between the Au NW and the Au film in the SNOF system. The incident light excites the surface plasmon of the NW, which in turn induces the surface plasmon polariton on the metal film. This surface plasmon polariton can be described as an image charge of the surface plasmon on the NW. The interaction between the surface plasmon and the surface plasmon polariton produces a gap mode of the electric field that becomes quite strong when the NW is close to the metal film, thereby producing a hot line; this picture is similar to the interpretation of Zheng and co-workers[27] and Aravind and Metiu[46] for the electric field enhancement of a sandwich nanostructure consisting of NPs on metal films. In contrast, the excitation of the surface plasmon of a Au NW on a Si substrate is extremely small, and only a weak electric field is generated around the surface of the NW. The theoretical results are fully consistent with the experimental observations.

For more quantitative assessment, the theoretical and experimental SERS enhancements of the SNOF with respect to the Au NW on a Si substrate are compared in Table 1. The squares of the electric field intensities, $|E|^4$, inside the SERS-active regions of the nanostructures are integrated within 10 nm of the surface of the Au NW in the two-dimensional cross section and then multiplied by 500 (the laser beam diameter is assumed to be 500 nm) to evaluate the theoretical SERS enhancement of the SNOF with respect to the Au NW on a Si substrate. This estimated enhancement agrees well with the experimental one.

The SERS enhancement of a SNOF is strongly dependent on the incident polarization direction, as in the case of a Ag NW on a Si substrate, for which the SERS signal was much weaker.[45] Figure 3a shows that a strongly enhanced SERS spectrum of BT adsorbed onto a Au/Au SNOF was observed for perpendicular polarization but that the SERS signal almost disappeared for parallel polarization. The polarization dependence of the SERS intensities of a SNOF were best-fit to $\cos^2\theta$ functions[42,47,48] (Figure 3b), as suggested by Nordlander and Xu.[49] A strongly enhanced electric field is induced at the gap between the NW and the film when perpendicularly polarized light impinges on the NW (Figure 3c and Figure S5 in the Supporting Information), but this enhancement is not induced by light with parallel polarization. The experimental and theoretical polarization-dependent SERS intensities of the SNOF are compared to those of the Au film in Table 2. The theoretical

(43) Stöckle, R. M.; Suh, Y. D.; Deckert, V.; Zenobi, R. *Chem. Phys. Lett.* **2000**, *318*, 131.
(44) Szafranski, C. A.; Tanner, W.; Laibinis, P. E.; Garrell, R. L. *Langmuir* **1998**, *14*, 3570.
(45) Barhoumi, A.; Zhang, D.; Tam, F.; Halas, N. J. *J. Am. Chem. Soc.* **2008**, *130*, 5523.
(46) Aravind, P. K.; Metiu, H. *Surf. Sci.* **1983**, *124*, 506.
(47) Tao, A. R.; Yang, P. *J. Phys. Chem. B* **2005**, *109*, 15687.
(48) Brolo, A. G.; Arctander, E.; Addison, C. J. *J. Phys. Chem. B* **2005**, *109*, 401.
(49) Wei, H.; Hao, F.; Huang, Y.; Wang, W.; Nordlander, P.; Xu, H. *Nano Lett.* **2008**, *8*, 2497.

SERS enhancement factor of the SNOF with respect to the flat Au film for perpendicular polarization is evaluated to be 8.2×10^4. The experimental enhancement factor is 5.9×10^3 (see the Supporting Information); this value is underestimated because it is calculated by a comparison with the noise intensity, which is the maximum possible signal from the flat Au film.

To further examine the polarization dependence of the SERS intensity, the center and tip of a NW were excited by light with perpendicular and parallel polarizations, respectively (Figure 4). Interestingly, for parallel-polarized light, the SERS enhancement at the tip is much stronger than at the center, but for perpendicularly polarized light, the SERS enhancements at the tip and the center are similar. This observation can be explained by the following interpretation. It is known that the plasmon on the metal surface can only be excited when the incident light has an electric field normal to the surface.[50] At the center of the NW, because the length of the NW ($\sim$10 μm) is much larger than the diameter of the laser spot ($\sim$500 nm), the parallel-polarized light cannot induce an electric field that is perpendicular to the NW surface.[42,49,51] At the tip of the NW, on the other hand, the electric field of the parallel-polarized light is normal to the surface curvature, and thus, the laser light can partially excite the localized surface plasmon and enhance the SERS intensity. A similar surface plasmon excitation at the NW tip has been reported previously by Sanders et al.[52] for the surface plasmon propagation of a Ag NW.

2. SERS Enhancement of SNOFs Composed of Different Materials. To investigate the dependence of the SERS enhancement on the material composition of the SNOF, we measured SERS spectra of BT for four distinct SNOF structures: (a) a Ag NW on a Ag film (Ag/Ag SNOF), (b) a Ag NW on a Au film (Ag/Au SNOF), (c) a Au NW on a Ag film (Au/Ag SNOF), and (d) a Au/Au SNOF. Figure 5 shows that the SERS intensity of a Ag/Ag SNOF is similar to that of a Ag/Au SNOF but $\sim$2 times larger than those of the Au/Ag and Au/Au SNOFs. Since SNOFs having a Ag NW show stronger SERS enhancements than SNOFs with a Au NW, it would be reasonable to assume that the SERS enhancement of a SNOF is more dependent on the material of the NW than on that of the film. This implies that the surface plasmon excitation on the NW is the more important step for the SERS enhancement and that the induction of the image charge on the metal film is similar for Au and Ag films.

3. Reproducibility and Stability of SERS Enhancement of the SNOF. Reproducibility and stability of SERS signals from a SERS-active platform are highly important properties for an optimum sensor. First, we tested the signal reproducibility at different positions on the SNOF. Figure 6a shows that the SERS spectra taken at five different positions on the same Au NW are fairly consistent in intensity and shape, indicating that the hot spots are uniformly created along the gap between the NW and the film. Second, we tested the reproducibility for different Au NWs on the Au film. The intensity variations in the SERS spectra taken from 20 Au NWs and a histogram of the intensities of 1000 cm^{-1} band indicate decent reproducibility (Figure 6b). The slight intensity fluctuations may be ascribed to variations in NW diameters, local film structures, and the adsorption of analyte on the NWs. Finally, we tested the stability over time by recording signals at 1 min intervals for 10 min at the same point on a Au NW. Figure 6c shows the measured SERS spectra and the time variation of the intensity of 1000 cm^{-1} band. The SERS signal is quite stable for 10 min, demonstrating good time stability.

Conclusion

In summary, we have reported the development of a novel SERS platform, the single nanowire on a film (SNOF), which can be constructed simply by placing a metallic NW on a metallic film. Optical excitation of this sandwich nanostructure provides a line of SERS hot spots at the gap between the NW and the film. The Au/Au SNOF provides reliable reproducibility, good time stability, and excellent sensitivity. A sensor of very small size (a few micrometers) employing this SNOF structure can be fabricated. By individual modification of the surface of several NWs and their combination together on the same film, multiplex nanobiosensing would be possible.[53]

Acknowledgment. This research was supported by KOSEF through NRL (ROA-2007-000-20127-0), SRC through the Center for Intelligent Nano-Bio Materials (R11-2005-008-03001-1-0) MEST through Center for Nanostructured Materials Technology (08K1501-02210), and Creative Research Initiatives (Center for Time-Resolved Diffraction) of MOST/KOSEF. Q-H.P. was supported by KRF/KOSEF.

Supporting Information Available: Theoretical studies for understanding SERS enhancement of SNOFs. This material is available free of charge via the Internet at http://pubs.acs.org.

JA807455S

(50) Knoll, W. *Annu. Rev. Phys. Chem.* **1998**, *49*, 569.
(51) Lee, S. J.; Baik, J. M.; Moskovits, M. *Nano Lett.* **2008**, *8*, 3244.
(52) Sanders, A. W.; Routenberg, D. A.; Wiley, B. J.; Xia, Y.; Dufresne, E. R.; Reed, M. A. *Nano Lett.* **2006**, *6*, 1822.
(53) Qin, L.; Banholzer, M. J.; Millstone, J. E.; Mirkin, C. A. *Nano Lett.* **2007**, *7*, 3849.